Contrib Mineral Petrol
DOI 10.1007/s00410-010-0570-7

ORIGINAL PAPER

Trace element partitioning between mica- and amphibole-bearing garnet lherzolite and hydrous basanitic melt: 2. Tasmanian Cainozoic basalts and the origins of intraplate basaltic magmas

John Adam · Trevor Green

Received: 10 October 2008 / Accepted: 4 August 2010

Abstract Oligocene volcanics from Oatlands in Tasmania, Australia, include olivine tholeiites, alkali olivine basalts, nepheline basanites and olivine nephelinites. They have compositional characteristics that are typical of intraplate basalts worldwide. They are generally enriched in incompatible elements relative to the primitive mantle and are strongly enriched in Nb, Ta and light rare earths, but not heavy rare earths. At the same time, they have Sr and Nd isotope compositions that are similar to those in some incompatible-element-depleted mid-ocean ridge basalts (E-type MORB). Experimentally obtained mineral/melt partition coefficients for an Oatlands basanite allow the relative concentrations of incompatible elements in the volcanics to be produced by small degrees of melting ($\leq$1%) of a source similar to the E-type MORB source of Workman and Hart (2005). However, the absolute concentrations that can be achieved in this way are much less than present in the most incompatible-element-enriched basanites and nephelinites at Oatlands. This contradiction can be explained by open-system melting under the influence of a conductive geotherm. This would have involved upwardly migrating near-solidus melts from the asthenosphere cooling along a sub-adiabatic geotherm. Cooling of the melts would have caused them to re-crystallize and accumulate in the overlying mantle, thereby enriching both the new host rocks and any residual melts in incompatible elements. This would also have increased the buoyancy of the host rocks leading to upwelling and further (decompression) melting of incompatible-element-enriched peridotite. We were able to use our partition coefficients to quantitatively model the development of incompatible-element enrichments in the Oatlands magmas by these processes. Our explanation is consistent with the characteristically scattered but widespread distributions and long time scales of intraplate volcanism in a broad variety of tectonic settings. This is because the conditions required to initiate volcanism (i.e. those of near-solidus melting of the asthenosphere) are relatively easy to produce and can therefore be caused by both near-surface tectonics and deeper mantle processes. Furthermore, the super-enrichments of incompatible elements in some intraplate volcanics can be attributed to the influence of normal geothermal gradients on melting processes. Without the very strong fractionation imposed by this combination of factors, the Oatlands volcanics would more closely resemble mid-ocean-ridge basalts.

Keywords Cainozoic · Intraplate volcanism · Basanite · Nephelinite · Tholeiite · Trace elements · Metasomatism · Open-system melting

Communicated by T. L. Grove.

J. Adam (✉) · T. Green
ARC National Key Centre for the Geochemical Evolution and Metallogeny of Continents, Department of Earth and Planetary Sciences, Macquarie University, Sydney, NSW 2109, Australia
e-mail: john.adam1@bigpond.com

Introduction

Intraplate basalts represent a compositional class of igneous rocks that (in spite of their name) are produced in a diverse range of tectonic settings (being absent only from mid-ocean ridges). They are typically enriched in incompatible minor and trace elements in spite of their being derived from sources that appear (on the basis of Sr and Nd isotope evidence) to have been depleted in these components relative to the primitive mantle (see Sun and McDonough 1989; Weaver 1991). They also display no

Published online: 21 August 2010

obvious compositional dependence on the tectonic environment in which they are produced (see Zindler and Hart 1986; Knutson et al. 1989). Because of these features, enquiries into the origin of intraplate basaltic magmas need both a holistic approach and the examination of specific circumstances. However, this twofold strategy has been relatively uncommon, partially because of the semantic association with plate interiors. Thus, intraplate magmatism has often been considered synonymous with hot-spot magmatism.

In this study, we investigate the problem of intraplate basaltic magma genesis by first examining a small group of (non-hot-spot related) intraplate volcanics (from Oatlands in Tasmania, Australia) for which we have an unusually comprehensive and specific data set (including high-pressure liquidus phase relationships, mineral/melt partition coefficients, thermo-barometric data from mantle xenoliths, major and trace element data, Sr and Nd isotope analyses, and a well studied regional context). We then consider our findings within the global context of intraplate volcanism, bearing in mind that key aspects of local magma production must be common to intraplate magmatism everywhere. These features must be such that they can impose a recognizable imprint upon magmas from compositionally variable sources and diverse tectonic settings.

The study area

The basalts described in this study are from the Oatlands district of southeastern Tasmania, Australia. They are of Late Eocene to Oligocene age and occur as small and isolated flow remnants within an early Tertiary graben (see Berry and Banks 1985). The basalts are one of the southernmost expressions of a volcanic province that extends discontinuously across eastern Australia, from Tasmania to Cape York (see Johnson 1989). Volcanism within this province includes a central-volcano type, which is thought to be hot-spot related, and a separate lava-fields type which is unrelated to hot-spot activity (see Duncan and McDougall 1989). Volcanism in the Oatlands district belongs to the lava-field type. This type is characterized by mafic volcanics of varying alkalinity (see Cas 1989). Individual provinces are typically of modest volume (up to 1500 km^3, but usually much less) and lateral extent (Duncan and McDougall 1989) with ages ranging from about 70 million years (Ma) to recent. Unlike for central volcanoes, lava field ages do not correlate with latitude (Duncan and McDougall 1989). Most dated basalts in the Oatlands district (including all of the alkaline samples) range in age from 27.6 to 24.3 Ma, with one older sample dated at 36.3 Ma (Sutherland 1984; Sutherland and Wellman 1986).

Sample descriptions and localities

The samples selected for analysis include most of those previously analysed by Adam (1990). They were collected from four different volcanic centres within the Oatlands district (Bow Hill, Vincent's Hill, Rose Hill Farm and Andover) and include olivine nephelinites, nepheline basanites, alkali olivine basalts and an olivine tholeiite. The basalts are all dense and very fine-grained with only a few percent or less of olivine and clinopyroxene microphenocrysts. All contain mantle-derived xenoliths and xenocrysts. The basalts at Bow Hill are especially rich in megacrysts, which include clinopyroxene, orthopyroxene (included in olivine), olivine and spinel. The Bow Hill volcanics are also distinguished by rare xenoliths of garnet-spinel-lherzolite and garnet-spinel-websterite (Sutherland et al. 1984).

The major-element compositions of the samples are given in Adam (1990). All have mafic compositions with from 8.5 to 12.0 wt.% MgO. In spite of relatively high K_2O concentrations in some examples (up to 2.2 wt.%) the volcanics are sodic in character (with K/Na <0.5). The nephelinites and basanites are also unusually rich in P_2O_5 (up to 1.49 wt.%) and total alkalis (up to 6.7 wt.%) for their SiO_2 and MgO concentrations.

One of the basalts (a nepheline basanite, UT-70489 from Bow Hill) was previously the subject of an experimental near-liquidus study by Adam (1990) who determined liquidus conditions of garnet lherzolite saturation at about 2.6 GPa and 1200°C, with 4.5 wt.% of dissolved H_2O and 2.0 wt.% of dissolved CO_2. More recently, the same basanite was used in an experimental study by Adam and Green (2006) who determined mineral/melt partition coefficients for minor and trace elements in near-liquidus garnet lherzolite phases and volatile-rich basanitic melt.

During this present study, both UT-70489 and other sampled basalts from Oatlands were analysed by solution ICP-MS for the same minor and trace elements studied by Adam and Green (2006). A number of samples were also analysed for Sr and Nd isotopes.

Analytical methods

Solution ICP-MS

All samples were analysed for Li, Rb, Cs, Be, Sr, Ba, Ga, In, Sn, Pb, Sb, Bi, Sc, Y, Ti, Zr, Hf, Nb, Ta, V, Cr, Mo, W, Co, Ni, Cu, Ag, Zn, Cd, La, Ce, Pr, Nd, Sm, Eu, Gd, Tb, Dy, Ho, Er, Yb, Lu, Th and U by inductively coupled plasma mass spectrometry (solution ICP-MS) using a Perkin Elmer Sciex Elan 6000 and an Agilent HP4500 in the GEMOC Geochemical Analysis Unit, Department of

Earth Sciences, Macquarie University, Australia. All samples were ground in an agate tema mill. The analytical procedures, including solution preparations, use of standards, and corrections for mass-dependent variations in instrument sensitivity, were essentially the same as those described by Eggins et al. (1997). In brief, samples were digested in concentrated HF-HNO_3 solutions. Following digestion and drying, samples were refluxed in 6 N HNO_3 to remove residual F. After again being dried they were re-dissolved in concentrated HNO_3 and diluted with H_2O preparatory to ICP-MS analysis. At this same time, samples were also doped with known weights of internal standard solutions. The latter contained a spectrum of artificially enriched isotopes that were used to monitor variations in mass-dependent instrument sensitivity (see Eggins et al. 1997). All analyses used a single-point calibration against the USGS standard BCR-2. Together with BHVO-2, BCR-2 was also periodically run as an unknown during the analysis of the Oatlands samples.

Sr and Nd isotopes

Sr and Nd isotopes were analysed using a Finnigan Triton thermal ionization mass spectrometer (TIMS) in the GEMOC Geochemical Analysis Unit, Department of Earth Sciences, Macquarie University, Australia. All of the acids used for sample digestion and chemical separation were sub-boiling distilled twice in Teflon® bottles. The digestion method used was standard hotplate dissolution in a 15-ml screw-cap Savillex® beaker. One hundred milligrams of rock powder were weighed into the beaker with equal volumes of 48% HF and 16 N HNO_3 and then dissolved on a hotplate for 48 h at 130°C. After digestion, samples were dried overnight on a hotplate at ~130°C, and then sufficient concentrated $HClO_4$ was added to cover the sample. The sample was dried down again overnight at 190°C before being reconstituted in 6.0 ml of 6 N sub-boiled HCl and re-dissolved for 24 h at 130°C. The sample was then taken up in 1.4 ml of a mixture of 2.5 N HCl:0.1 N HF ready to be loaded onto the cation exchange column.

Strontium and neodymium were purified from the same solution using 2 columns. A standard cation exchange column of Biorad AG50 W-X8 resin (200–400 mesh) was used to separate Sr and REE from the matrix (including Rb). The REE fraction was then passed through an Eichrom Ln.spec resin (50–100 particle size) column to separate Nd from Ba and LREE (La, Ce, Pr and Sm) following the method of Pin et al. (1997).

Sr and Nd compositions were measured in static mode multi-collection with relay matrix rotation (the "virtual amplifier" of Finnigan) on a single Re and double Re filament, respectively. A single analysis typically consisted of 200 cycles (10 blocks of 20) to allow a full rotation of the virtual amplifier. The data were corrected for mass fractionation using $^{86}Sr/^{88}Sr = 0.1194$ and $^{146}Nd/^{144}Nd = 0.7219$, respectively.

XRF analyses of halogens

Cl, Br and I were analysed using X-ray fluorescence spectrometry on pressed pellets using a Spectro XLAB 2000 energy dispersive spectrometer, housed in the GEMOC Geochemical Analysis Unit, Department of Earth Sciences, Macquarie University, Australia.

Results

Reproducibility and accuracy

Duplicate ICP-MS analyses of the nepheline basanite UT-70489 (Table 1) agree within ±3% for most elements. The largest relative variations are for Ag (6%) and Cd (8%), both of which have low absolute concentrations (4.0 and 0.11 ppm, respectively). For the replicate analyses of BCR-2 and BHVO-2 (Table 1) relative one sigma standard deviations (for $n = 4$) are generally within ±3% of average values, and frequently within ±1%. Larger deviations occur for Yb, Lu, Hf, Ta, W, Pb, Th and U (4–10%), as well as for Cd, Tl and Bi (46–57%). The last three have very low absolute concentrations (0.01–0.38 ppm). With few exceptions, the average values obtained for BCR-2 and BHVO-2 as unknowns agree (within the previously described uncertainties) with the preferred values used for these reference materials at GEMOC.

The accuracy and precision of $^{86}Sr/^{88}Sr$ and $^{143}Nd/^{144}Nd$ measurements is demonstrated by analyses of the NIST SRM 987 Sr standard ($^{86}Sr/^{88}Sr = 0.710257 \pm 35$ (2 sd; $n = 13$)) and JMC Nd standard ($^{143}Nd/^{144}Nd = 0.511106$ 10 (2 sd; $n = 19$)), made over a period of 2 years. USGS reference material BHVO-2 was processed with the samples analysed in this study and gave values of $^{86}Sr/^{88}Sr = 0.703507 \pm 8$ (2se)) and $^{143}Nd/^{144}Nd = 0.512968 \pm 4$ (2se)). These values are within the long-term average values produced at GEMOC: $^{86}Sr/^{88}Sr = 0.703490 \pm 28$ (2 sd; $n = 17$) and $^{143}Nd/^{144}Nd = 0.512967 \pm 28$ (2 sd; $n = 13$).

Incompatible-element concentrations in the Oatlands Volcanics

Concentrations of trace and minor elements in the Oatlands samples are given in Table 1. On mantle-normalized plots (Fig. 1), they show patterns of incompatible-element enrichment that are typical of intraplate basalts worldwide. Concentrations increase progressively from Lu to Nb, and then decrease from U to Cs. More particularly, Nb and Ta

Table 1 Analysed trace and minor element concentrations (in ppm) in samples of Oatlands volcanics, and in USGS standards BCR-2 and BHVO-2

Locality	Bow Hill				Vincent's Hill			RHF	Andover	BCR-2		BHVO-2	
Sample number	489a	489b	490	491	493	494	492	495	497	$n = 4$		$n = 4$	
Li6	5.0	5.0	4.4	4.7	4.4	4.1	3.5	2.2	1.9	3.9	(0.1)	1.8	(0.1)
Be9	4.3	4.3	4.2	4.2	3.9	3.5	2.6	2.5	1.0	2.66	(0.04)	1.19	(0.02)
Sc45	13.4	13.3	12.5	12.9	18.6	17.2	20.3	18.1	22.7	33.5	(0.7)	30.8	(1.0)
Ti49	14,340	14,592	16,795	17,546	19,332	17,305	17,999	16,895	10,724	13,491	(135)	16014	(514)
V51	122	124	129	136	165	151	168	114	144	396	(3)	291	(11)
Cr53	491	494	290	265	319	298	227	321	348	16.6	(0.2)	308	(10)
Co59	46	46	47	47	51	47	53	57	50	36.2	(0.4)	42.7	(1.1)
Ni60	332	339	238	208	229	222	198	439	225	13.4	(0.2)	123.9	(1.5)
Cu65	68	70	66	65	77	60	67	105	73	27.0	(0.3)	166.6	(2.7)
Zn66	157	159	167	167	157	142	141	143	103	124	(2)	101	(1)
Ga71	21.7	21.6	25.9	26.3	23	20.7	21.2	22	17.6	21.1	(0.0)	20	(0.7)
Rb85	28.5	28.8	35.6	34.3	23.6	27	19.9	30.2	9.9	46.8	(0.6)	9.1	(0.2)
Sr86	1542	1566	1396	1428	1185	1172	847	789	323	332	(5)	383	(13)
Y89	38.2	38.4	38	38.6	40.3	40.3	35.4	39	22.8	38.4	(0.5)	27.3	(0.7)
Zr90	512	514	504	520	517	488	336	338	119	194	(2)	174	(5)
Nb93	143	146	146	148	132	129	89	76	21	12.5	(0.3)	18.8	(0.3)
Mo95	4.6	4.7	4.5	4.4	4.6	5.9	4.4	3.6	1.3	248	(4)	4.0	(0.1)
Ag107	3.9	4.1	4.0	4.2	3.8	3.7	2.5	2.8	1.0	1.6	(0.07)	1.54	(0.04)
Cd111	0.11	0.12	0.11	0.11	0.11	0.12	0.07	0.09	0.04	0.22	(0.09)	0.08	(0.04)
In115	2.2	2.2	2.4	2.5	2.2	2.2	2.0	2.1	1.5	2.04	(0.04	1.87	(0.01)
Sn118	4.7	4.7	4.8	4.9	4.1	4.1	2.9	3.6	2.4	2.69	(0.01)	2.39	(0.02)
Sb121	0.11	0.11	0.19	0.1	0.11	0.25	0.07	0.06	0.03	0.29	(0.01)	0.07	(0.00)
Cs133	0.60	0.60	0.70	0.58	0.62	0.67	0.42	0.39	0.27	1.20	(0.01)	0.1	(0.00)
Ba135	702	709	637	646	552	576	344	401	127	665	(7)	132	(1)
La139	97	96	92	93	86	87	59	50	14	25.0	(0.2)	15.7	(0.2)
Ce140	194	195	189	193	176	174	122	105	30	52.1	(0.4)	38.3	(0.2)
Pr141	22.6	22.9	22.7	23.0	21.1	21.4	15.0	13.1	3.9	6.9	(0.08)	5.6	(0.1)
Nd146	87.6	87.8	88.7	89.8	81.5	83.3	59.8	52.8	17.0	28.5	(0.2)	25.1	(0.1)
Sm147	17.0	17.3	17.6	17.9	15.4	15.9	11.9	11.3	4.5	6.61	(0.03)	6.31	(0.05)
Eu153	5.41	5.42	5.56	5.65	4.78	4.81	3.76	3.77	1.65	2.06	(0.02)	2.17	(0.01)
Gd157	15.0	15.2	15.6	15.8	13.6	14.0	10.9	10.9	4.9	6.83	(0.04)	6.46	(0.03)
Tb159	1.93	1.92	1.98	2.01	1.79	1.85	1.49	1.53	0.78	1.08	(0.01)	0.99	(0.00)
Gd160	14.0	14.1	14.7	14.9	12.8	13.2	10.5	10.5	5.0	6.83	(0.03)	6.5	(0.02)
Dy163	8.77	8.84	9.03	9.13	8.63	8.97	7.4	7.76	4.36	6.3	(0.02)	5.42	(0.02)

Table 1 continued

Locality	Bow Hill				Vincent's Hill			RHF	Andover	BCR-2		BHVO-2	
Sample number	489a	489b	490	491	493	494	492	495	497	$n = 4$		$n = 4$	
Ho165	1.43	1.44	1.44	1.45	1.5	1.58	1.33	1.4	0.83	1.31	(0.00)	1.04	(0.00)
Er167	3.12	3.14	3.04	3.07	3.55	3.73	3.21	3.39	2.15	3.66	(0.00)	2.64	(0.01)
Yb173	1.7	1.74	1.58	1.61	2.3	2.42	2.14	2.33	1.48	3.17	(0.17)	1.74	(0.15)
Lu175	0.2	0.21	0.19	0.19	0.3	0.32	0.29	0.31	0.21	0.47	(0.03)	0.24	(0.02)
Hf178	10.0	10.3	10.0	10.5	9.9	9.7	6.9	6.9	2.7	4.6	(0.3)	6.1	(4.8)
Ta181	8.2	8.5	8.5	8.8	7.7	7.7	5.1	4.3	1.2	0.7	(0.1)	14.5	(0.0)
W184	1.92	1.96	1.39	1.32	1.91	2.19	2.12	1.85	0.68	0.9	(0.1)	14.5	(0.0)
Pb206	4.82	4.93	4.61	4.43	5.07	4.82	2.82	2.61	1.31	9.86	(0.66)	1.41	(0.11)
Pb208	4.67	4.73	4.45	4.28	4.9	4.69	2.74	2.48	1.26	9.82	(0.69)	1.4	(0.11)
Bi209	0.01	0.01	0.01	0.01	0.01	0.02	0.01	0.01	0.01	0.03	(0.02)	0.01	(0)
Th232	11.79	11.96	10.54	10.81	10.77	10.56	6.85	5.48	1.68	5.82	(0.38)	1.1	(0.09)
U238	3.42	3.54	3.12	3.25	3.13	3.28	2.05	1.62	0.47	1.59	(0.1)	0.37	(0.03)
Cl	1240		981	1001	906	984	506	562	205				
Br	2.9		2.5	2.23	1.7	2.2	1.1	1.3	0.2				

Analyses were by solution ICP-MS except for Cl and Br which were by XRF. I was also analysed by XRF but was below detection limits ($\sim$1 ppm) in all samples

Numerical suffixes to elements indicate the mass of the isotope analysed

Figures in parentheses are 1σ standard deviations for replicate analyses of BCR-2 and BHVO-2

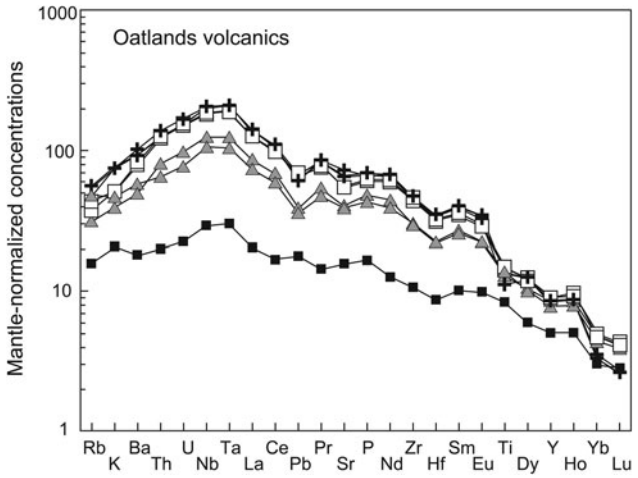

Fig. 1 Mantle-normalized incompatible-element concentrations in the Oatlands volcanics. *Crosses* represent basanites and nephelinites from Bow Hill. *Open squares* represent basanites from Vincent's Hill. *Grey triangles* represent alkali olivine basalts from Vincent's Hill and Rose Hill Farm. *Filled squares* are for the Andover olivine tholeiite. The normalization values used are from McDonough and Sun (1995)

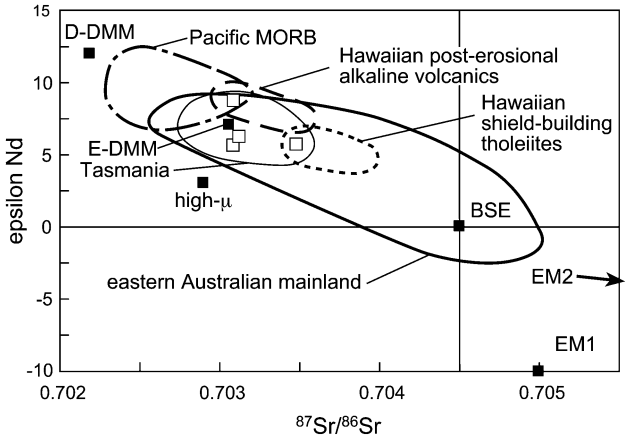

Fig. 2 $^{143}Nd/^{144}Nd$ versus $^{87}Sr/^{86}Sr$ in selected Oatlands volcanics with the fields of Pacific MORB, other eastern Australian lava fields, and selected Hawaiian volcanics shown for comparison. The D-DMM, E-DMM and BSE values are from Workman and Hart (2005). The high-μ value is based on estimates presented by Zindler and Hart (1986). Values for Pacific MORB are from Ito et al. (1987), Ferguson and Klein (1993), Pyle et al. (1995) and Kamenetsky et al. (2000); east Australian lava field data are from McDonough et al. (1985), Wilkinson and Hensel (1991), O'Reilly and Zhang (1995), Zhang and O'Reilly (1997), and Zhang et al. (2001). Data for Hawaiian post-erosional alkaline volcanics (North Arch and Honolulu Volcanics) and shield-building tholeiites (Mona Loa and Kilauea volcanoes) are from Roden et al. (1984), Chen et al. (1996), Cohen et al. (1996) and Frey et al. (2000)

are enriched relative to La, a feature identified by Weaver (1991) as characteristic of high-μ type intraplate magmas. When compared to examples from many other continental as well as ocean island settings (e.g. Clague and Frey 1982; Schminke 1982; Wedepohl 1985; Barker et al. 1987; O'Reilly and Zhang 1995; Aldanmaz et al. 2006), the incompatible-element enrichments in the Oatlands samples are at the upper limit of concentrations found in sodic intraplate basalts of similar SiO_2 and MgO content. Compared with values compiled by Pfänder et al. (2007), Nb/Ta and Zr/Hf are also strongly fractionated. All of the samples, excepting the Andover tholeiite, have negative Pb anomalies.

Sr and Nd isotopes

Sr and Nd isotope ratios for individual samples are shown in Table 2. They partially overlap with data for Hawaiian tholeiitic and alkaline volcanism and include some of the lowest $^{87}Sr/^{86}Sr$ and highest $^{143}Nd/^{144}Nd$ so far measured in eastern Australian Cainozoic basalts (Fig. 2). They also have a small range of variation which clusters close to the E-type mid-ocean ridge basalt source composition (E-DMM) estimated by Workman and Hart (2005). This composition is close to the Prevalent Mantle (or PREMA) composition of Zindler and Hart (1986). The Oatlands samples are thus included within a broad but approximately linear array of $^{87}Sr/^{86}Sr$ and $^{143}Nd/^{144}Nd$ variations defined by Pacific Ocean MORB, east Australian Cainozoic lava fields and the primitive mantle. This array encompasses much of the isotopic variation found in intraplate basalts globally (see Zindler and Hart 1986; Weaver 1991).

Table 2 Sr and Nd isotopes in Oatlands samples

	$^{87}Sr/^{86}Sr$	$^{143}Nd/^{144}Nd$	εNd
UT-70489	0.703122 (6)	0.512959 (8)	6.3
UT-70493	0.703092 (7)	0.512930 (7)	5.7
UT-70495	0.703092 (6)	0.513083 (8)	8.7
UT-70497	0.703531 (3)	0.512933 (13)	5.8

Figures in parentheses indicate absolute standard errors in the final significant figure(s)

Discussion

Inter-element correlations

For the purposes of this discussion, all element concentrations have been adjusted for the effects of olivine fractionation on original magma compositions (which are assumed to have had similar Fe/Mg). The amount of olivine fractionation was calculated in each case assuming $D_{Fe/Mg}^{olivine/melt} = 0.3$ (see Roeder and Emslie 1970) and Fe^{+3}/Fe total = 0.2 with the calculated liquidus olivine being added to magmas in 1% increments (with the melt composition being adjusted after each addition) until the liquidus olivine obtained *fo* = 87.6 (the liquidus olivine

composition for UT-70489). Although this step doesn't affect our conclusions, it noticeably improves some of the inter-element correlations that we discuss.

The concentrations of most incompatible elements are a negative linear function of SiO_2. But when plotted against other incompatible elements, the trends for most incompatible elements are positive and either linear or curvilinear (Fig. 3). In cases where elements have similar incompatibility (e.g. La and Nb), these trends can usually be interpolated through the origin. But for a few elements (e.g. K, Ti and Lu) the trends are less obviously linear and/or less likely to extend through the origin. The concentrations of most compatible elements (e.g. V) are relatively constant and do not vary systematically with SiO_2.

Magma formation by closed-system melting of a peridotite source

The generally co-linear patterns of element variation in the Oatlands volcanics are typical of intraplate basalt suites worldwide (e.g. Frey et al. 1978; Clague and Frey 1982; Hofmann and Feigenson 1983; Ormerod et al. 1991; Aldanmaz et al. 2006). Such trends have usually been attributed to variable degrees of batch melting during decompression melting of a common peridotite source (e.g. op. cit.). When melting occurs in this way, the degree of melting is inversely related to pressure (see Green and Liebermann 1976; Green 1989). Thus, nephelinitic magmas are produced by relatively small degrees of melting (a few %) at high pressures (>2.5 GPa), whereas tholeiitic magmas are produced by the highest degrees of melting (≥20%) at relatively low pressures (<2.0 GPa). Other magma compositions are produced by intermediate degrees of melting and at intermediate pressures.

Although mantle melting is now understood to be a more complex process than the mechanism just described, both the compositional data and partition coefficients for the Oatlands samples (Table 3) are surprisingly consistent with the simple decompression batch-melting model. This can be seen in Fig. 4a where the calculated concentrations of incompatible elements in modal batch-melts of a pyrolite-based Oatlands source are plotted for comparison with concentrations in the natural volcanics. Incompatible-element concentrations in the pyrolite source were calculated using the approach of Frey et al. (1978). This first involved the estimation of a source mode from mass balances between major-element concentrations in UT-70489 and its near-liquidus phases (with Mg/Fe in all phases adjusted to that of pyrolite) and those in Ringwood's (1966) pyrolite [this mode contained (by weight) 5.5% basanite +1% phlogopite +4% garnet +14% clinopyroxene +19% orthopyroxene +56.5% olivine]. Partition coefficients (Table 3) were then used to calculate the concentrations of incompatible minor and trace elements in individual mineral phases. Concentrations in the bulk source (see Fig. 7) could then be calculated from these values and the previously calculated source mode.

Although the modal batch-melting trends reproduce variations in the natural volcanics quite well for most elements, the physics of melt extraction are thought to make batch melting unlikely (see McKenzie 1984). Instead, melts are thought to begin migrating from their source rocks almost as soon as they form. This results in fractional melting rather than batch melting. A problem with this conclusion is that fractional melting (Fig. 4a) produces compositional trends that are very different from those of the natural volcanics. This is true even when allowance is made for the accumulation and averaging of partial-melts in a separate reservoir (i.e. accumulative fractional melting). However, if a fraction of retained melt is allowed during melting (fractional melting with some retained melt) the fractional melting trends begin to approach those produced by batch melting. With approximately 5% retained melt, the trends for most elements are close to those produced by the natural data (Fig. 4b).

For the few elements that are not well reproduced by the batch-melting model (e.g. Na, Cs, Ti and Lu), a number of explanations can be offered. One is non-modal melting and the retention of these elements in minor phases that are preferentially consumed by melting (e.g. amphibole, mica, garnet and Fe–Ti-oxides). Thus, the presence of mica in early melting residues may explain the relatively low concentrations of K, Rb and Cs in nephelinites and basanites. Garnet preferentially retains HREE, but is destabilized by the decompression which drives melting. Thus, HREE concentrations in melts would initially have increased, but then been progressively diluted once garnet was removed by decompression and continued melting. Although residual amphibole and Fe-Ti-oxides offer a potential explanation for the behaviour of Ti and Na, they are not near-liquidus phases of UT-70489 [although mica possibly is] (see Adam 1990; Adam and Green 2006). Indeed, in the many near-liquidus experiments that we have conducted on natural alkaline basalts, Fe–Ti-oxides were crystallized only when the starting material had either been deliberately enriched in TiO_2 and/or the experiment was conducted at high fO_2 (buffered by haematite and magnetite). Thus, primary source heterogeneity is a more likely explanation for the inconsistent behaviour of Na_2O and TiO_2.

A final comment on potential residual phases concerns the role of sulphide. Variations in the concentrations of chalcophile elements (Cu, Zn, Ag and Pb) in the Oatlands samples are all consistent with partitioning between silicate phases alone. Thus, if sulphide was present in melting residues, its fraction is likely to have been small (<0.1%).

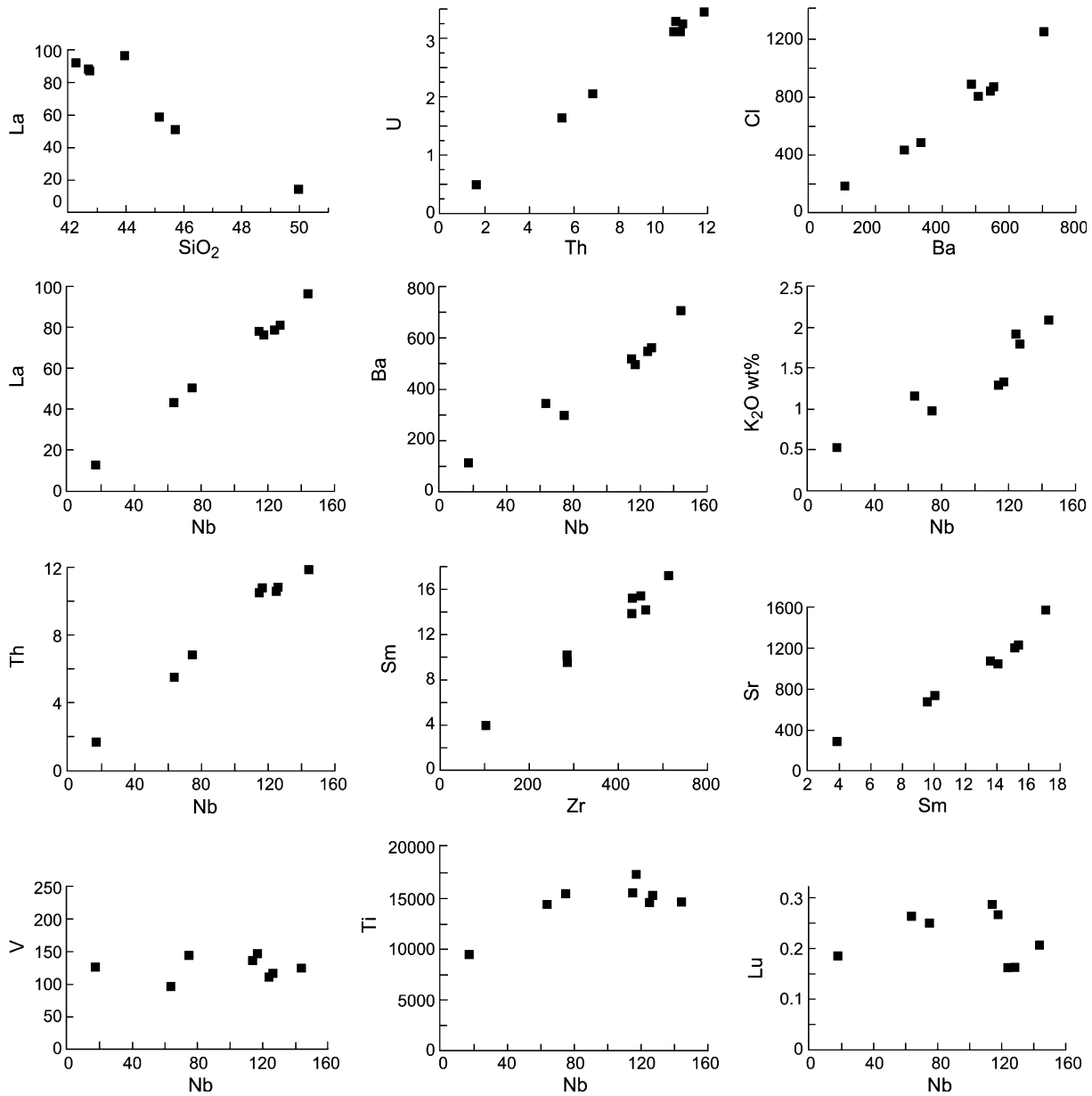

Fig. 3 Inter-element correlations in the Oatlands volcanics [data from Table 1, Adam (1990)]

In summary, our calculations show that an origin for the Oatlands magmas by decompression melting of a common peridotite source (that is similar to pyrolite) is at least broadly consistent with both compositional data and experimentally determined partition coefficients for the Oatlands volcanics. However, this source would have been strongly enriched in incompatible minor and trace elements relative to the primitive mantle (Fig. 7). None of the melting models tested so far could produce the inter-element trends of the Oatlands magmas from non-enriched sources. Enriched sources are in fact a typical conclusion whenever incompatible elements are used to infer the source characteristics of intraplate basaltic magmas (e.g. Sun and Hanson 1975; Frey et al. 1978, 2000; Clague and Frey 1982; Ormerod et al. 1991; Aldanmaz et al. 2006). This raises the familiar problem of how to explain Sr and Nd isotope ratios that are consistent with an incompatible-element-depleted source. One potential solution is open-system melting. During this type of melting, material can be both added and removed from the source as melting progresses. Depending on whether the added material is either crystalline or molten, open-system melting can also describe processes that are inherent to either dynamic melting or metasomatism.

Table 3 Partition coefficients used for the incompatible-element models discussed in this study

Run	1949	1950	1955	R80	1949	R77
°C	1160	1050	1190	1160	1160	1100
GPa	2.7	2.0	3.5	2.7	2.7	2.0
	mica	amph	garnet	cpx	opx	olivine
Rb	4.97	0.26	0.0002	0.000	0.0038	0.000
K	4.1	0.8				
Ba	3.1	0.19	0.0003	0.00016	0.0036	0.0001
Th	0.0004	0.0035	0.0006	0.006	0.0005	0.0002
U	0.0033	0.0039	0.0037	0.005	0.0003	
Nb	0.055	0.069	0.001	0.006	0.0007	
Ta	0.062	0.083	0.002	0.02	0.0008	
La	0.0004	0.05	0.0005	0.03	0.0006	
Ce	0.0003	0.09	0.0028	0.06	0.0017	
Pb	0.089	0.07		0.018		
Sr	0.16	0.23	0.032	0.08	0.002	
P	0.003	0.019	0.032	0.024	0.007	0.038
Nd	0.0009	0.20	0.027	0.15	0.004	
Sm		0.30	0.164	0.25	0.011	
Zr	0.012	0.13	0.145	0.10	0.010	0.001
Hf	0.015	0.27	0.108	0.20	0.017	0.0008
Ti	0.79	0.72	0.19	0.29	0.10	0.011
Tb	0.0007	0.40	1.18	0.38	0.03	0.001
Y	0.003	0.38	2.57	0.42	0.046	0.003
Ho	0.0009	0.41	2.59	0.43	0.048	0.003
Yb		0.27	4.54	0.43	0.077	
Lu	0.0017	0.30	4.66	0.41	0.09	0.024
Zn			1.61	0.31	0.66	0.88
In	0.14	1.09	10.33	0.52	0.24	0.09
Sn	0.05	0.72	0.86	0.12		0.002
Sb	0.0013	0.016		0.017	0.001	0.0004
Mo	0.05	0.03	0.003	0.016	0.004	0.001
Pb	0.089	0.07	0.018	0.02		
Ag	0.04		0.22	0.33		0.001
Cu		1.1	0.69	1.26	2.83	1.2

All values are from Adam and Green (2006)

Where figures are not given, it can be assumed that values are negligible

Amph amphibole, *cpx* clinopyroxene, *opx* orthopyroxene

Magma formation by open-system melting: (1) dynamic melting

Dynamic melting describes a situation in which both the melt and its residue move continuously, but at different rates, as melting progresses (see Richter 1986). In this way, melts may be affected by contact with a spectrum of melting residues over a range of pressures. Thus, melts formed by comparatively small degrees of melting at high pressures can contribute to the overall character of large-degree melts. The relative contributions of small-degree melts can also be increased by the horizontal segregation of residues from melts during melting and melt extraction. Eggins (1992b) suggested a three-dimensional mechanism of this kind to explain incompatible-element concentrations in plume-derived Hawaiian tholeiites. As noted by Richter (1986), complex melting processes that integrate the effects of multiple variables [(e.g. time, melt and matrix velocities, direction of travel, melting rates and distance (in 1, 2 or 3 dimensions)] can produce melts that appear to have been derived from an incompatible-element-enriched source, even though the source was not enriched.

In the case of the Oatlands magmas, the feasibility of dynamic melting can be tested by examining the limiting case of melt compositions produced by infinitesimally small degrees of melting of non-enriched sources. For dynamic melting to be a sufficient explanation of magma genesis, these melts must have incompatible-element concentrations that are at least equal to those in the most incompatible-element-enriched nephelinites and basanites at Oatlands. Two potential non-enriched sources are the primitive mantle (PM) of McDonough and Sun (1995) and the ''enriched'' depleted mid-ocean ridge basalt source (E-DMM) of Workman and Hart (2005). The first provides a reasonable upper limit on incompatible-element concentrations in a potential source, whereas the second provides a depleted source that is both sufficiently fertile with respect to basaltic components (Al_2O_3, CaO and Na_2O) and has Nd and Sr isotope ratios similar to those in UT-70489. It is also potentially available since it can be presumed to have a widespread distribution in the neighbouring sub-oceanic mantle. Source ratios of garnet, clinopyroxene, orthopyroxene and olivine were calculated from mass balances between major elements in the model sources and near-liquidus phases from UT-70489. The relative concentrations of FeO and MgO in all phases were also adjusted to equal those in the source peridotites. The partition coefficients used were from Table 3.

Incompatible-element concentrations in infinitesimal melts of both PM and E-DMM are shown normalized to PM concentrations in Fig. 5. The composition of UT-70489 is also shown for comparison. The calculated patterns reproduce some features of the natural basanite. Concentrations progressively increase from Lu to Nb. In the calculated partial-melt of E-DMM, there is also a relative decrease in concentrations from Nb to Rb. More minor comparisons are the duplication of the inflection between Zr and Sm, and the relative enrichments of Nb and Ta over La. In spite of these similarities, there are also significant differences. With the exception of the most highly incompatible elements (from Ta to Rb), absolute concentrations in the calculated melts are much lower than

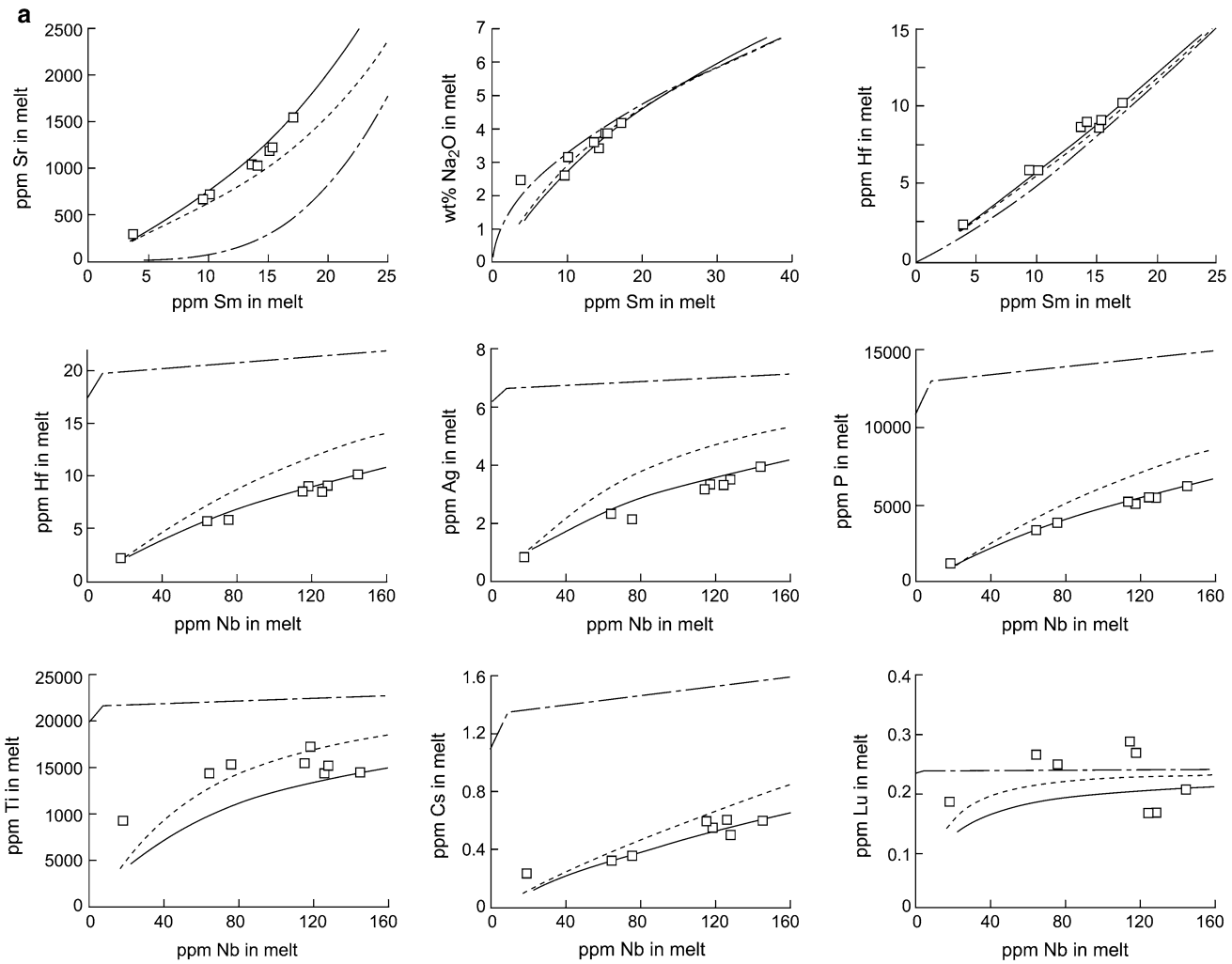

Fig. 4 **a** Inter-element correlations in melts produced by batch-melting (*solid lines*), fractional melting (*alternate long and short dashed lines*) and cumulative fractional melting (*short dashed lines*) of a pyrolite-based Oatlands source (see text for details). Data for the Oatlands volcanics (*open squares*) are also shown for comparison. Melt compositions were calculated using equations 7.9, 7.19, 7.20 and 7.24 of Shaw (2006). **b** The effect of retained melt was determined using the approach of Albarède (1995) who treated the retained melt as a separate phase with a partition coefficient equal to one. This allowed concentrations in escaping melts to be calculated using the fractional-melting and accumulative-fractional-melting equations

those in the basanite. This is especially true for the infinitesimal melt of E-DMM (which UT-70489 isotopically resembles). Another difference is that, unlike the natural basanite, the calculated melts have strongly fractionated Nb/Ta and Pb/Ce (with Nb/Ta and Pb/Ce $\gg$ PM). These features disappear as melting increases, but this also decreases absolute concentrations.

Following Frey et al. (1978), we also tested whether incompatible-element concentrations in the Andover tholeiite could be produced by small degrees of melting of unenriched peridotite. This allows us to more closely examine the consequences of the dynamic melting models proposed by Richter (1986) and Eggins (1992b). A partial match to the tholeiite is produced by a calculated 1% partial-melt of garnet-bearing E-DMM (Fig. 6). This provides a good fit to the concentrations of the more strongly incompatible elements, but under estimates HREE. A closer match to the HREE is possible with a smaller fraction of residual garnet (i.e. <10%) although some residual garnet is needed for a close co-incidence. If a PM source is chosen instead of E-DMM, from 3 to 5% melting is needed to reproduce the tholeiite's concentrations of Nb and LREE. In this case though, the overall pattern of the tholeiite (Fig. 6) is not as well reproduced because of overly high concentrations of Rb, K, Ba, Th and U.

When the results of the near-solidus melting calculations are applied to the dynamic melting models of Richter (1986) and Eggins (1992b), the following conclusions can be made:

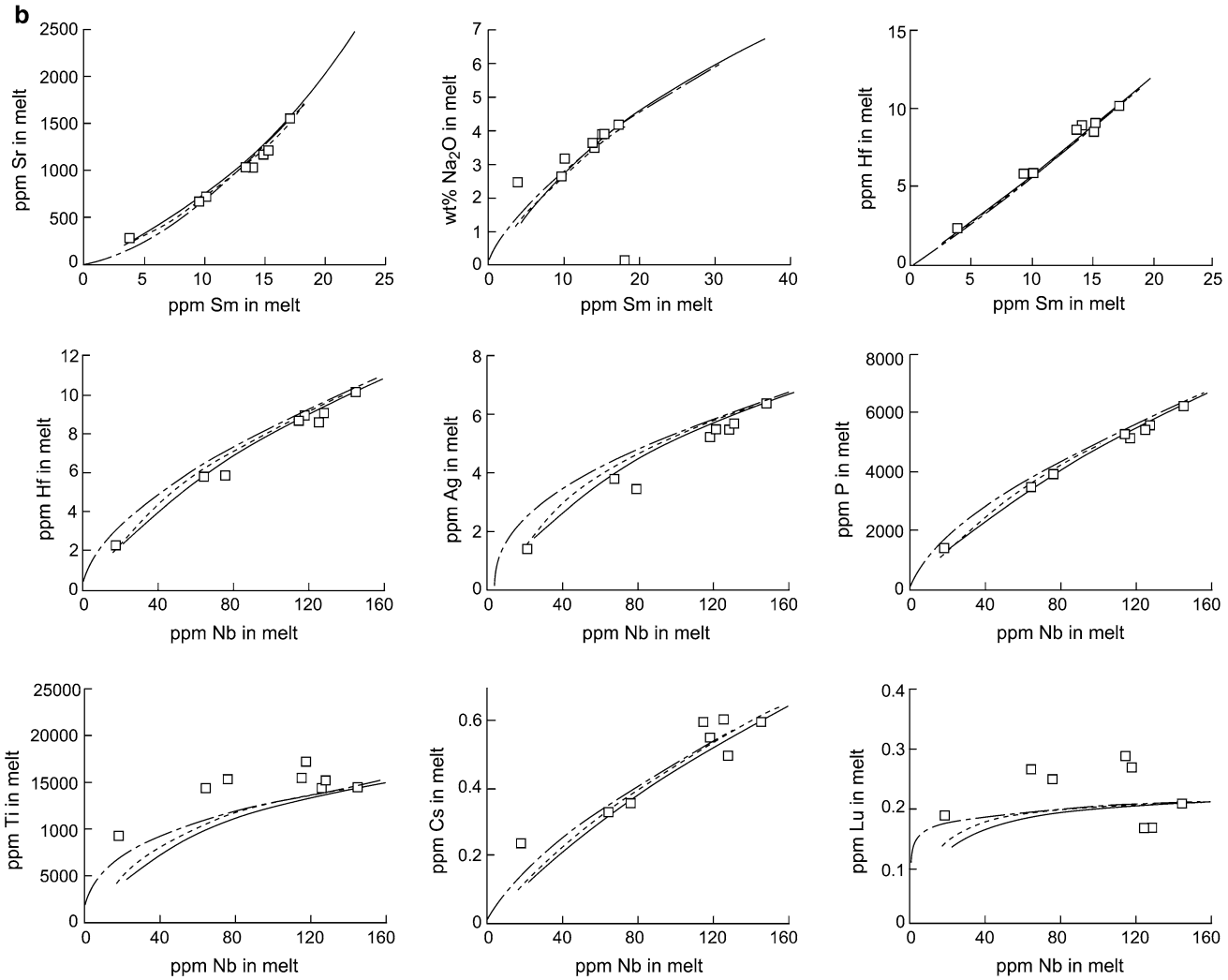

Fig. 4 continued

- Dynamic melting can be used to explain the compositional characteristics of the Andover tholeiite, but only if incompatible-element concentrations were completely dominated by the lowest melting-point fractions. These low-degree melts would need to have re-equilibrated with more refractory (harzburgite) residues at lower pressures (see Green and Ringwood 1967; Eggins 1992a; Wagner and Grove 1998).
- Although many of the compositional characteristics of the Bow Hill basanite can be reproduced by near-solidus melting of an unenriched peridotite source similar to E-DMM, the original basanite magma cannot have been produced in this way. It requires a source that was pre-enriched in incompatible elements. As a consequence, dynamic melting by itself cannot produce the compositional range of the Oatlands magmas.

Magma formation by open-system melting: (2) mantle metasomatism

The results of the preceding investigations suggest that, in spite of the Sr and Nd isotope compositions of erupted magmas, the Oatlands source must have been enriched in incompatible elements at the time of magma generation and segregation. But it is necessary to explain how these incompatible-element enrichments might reasonably have been produced. The usual explanation for this kind of problem is mantle metasomatism, a process by which the source is enriched in incompatible elements by migrating melts or fluids (see Varne 1970; Bailey 1982; Wright 1984; Halliday et al. 1995; Pilet et al. 2005). This situation can describe open-system melting where either some or all of the added melt is converted to crystals. In the case of the

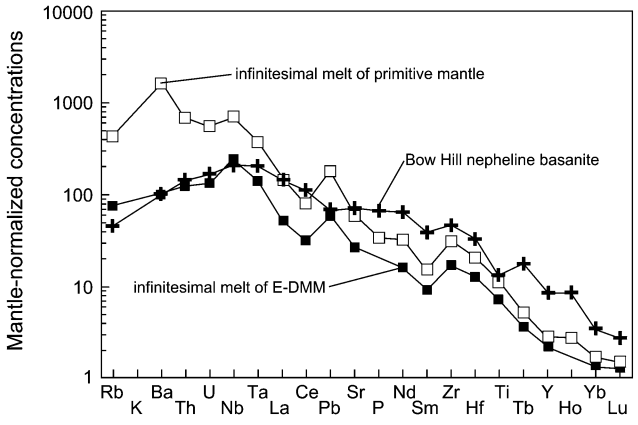

Fig. 5 Incompatible-element concentrations in infinitesimal melts of E-DMM and primitive mantle calculated using partition coefficients from Table 3. Primitive mantle concentrations are from McDonough and Sun (1995). E-DMM values are from Workman and Hart (2005)

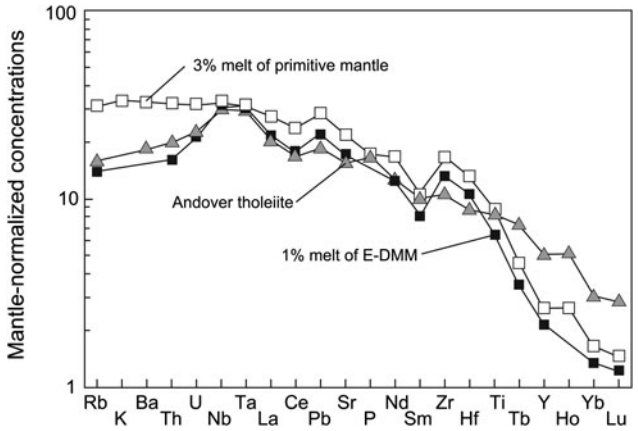

Fig. 6 Incompatible-element concentrations in a 1% partial melt of E-DMM and a 3% partial-melt of primitive mantle calculated using partition coefficients from Table 3. Primitive mantle concentrations are from McDonough and Sun (1995). E-DMM values are from Workman and Hart (2005)

Oatlands magmas, the added melt must have come from a source that *was* depleted. A potential source of this kind is the E-DMM. It is isotopically similar to the Oatlands samples (Fig. 2), is generally depleted in incompatible elements, and represents a widespread component of the neighbouring sub-oceanic mantle. In addition, we have already been able to show that it is capable of producing many of the trace and minor element characteristics of Oatlands magmas.

Figure 7 shows a model Oatlands source produced by the addition of 30% of a 0.7% partial-melt of E-DMM to an E-DMM protolith. This reproduces most features of the previous pyrolite-based Bow Hill source (Fig. 7). Some of the noticeable discrepancies (e.g. Sr, Ti, Sm, Tb and Ho) could reflect small differences in the modal proportions of

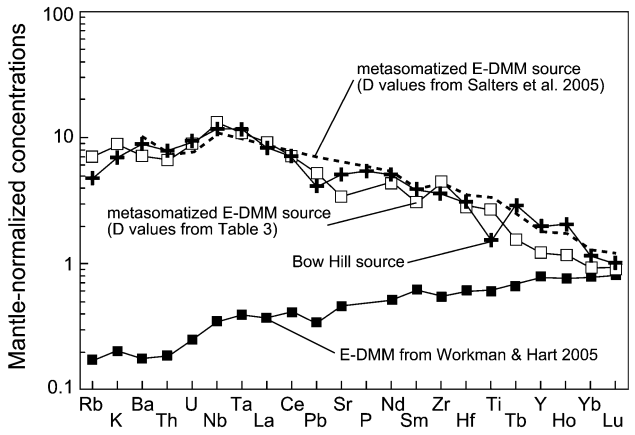

Fig. 7 Incompatible-element concentrations in a metasomatized source produced by the addition of 30% of a 0.7% melt of E-DMM to an E-DMM protolith (*open squares*). The partition coefficients used were from Table 3. Shown for comparison is a pyrolite-based source composition (*crosses*) calculated for the nepheline basanite UT-70489 (see text for more details). Also shown is a second metasomatized source composition produced by the addition of 30% of a 0.4% melt of E-DMM to an E-DMM protolith (*dashed line*). In this case melt concentrations were calculated using data (including partition coefficients) from Salters et al. (2002). The normalization factors are from McDonough and Sun (1995)

residual phases (e.g. mica and garnet). Misfits could also result from changes in mineral/melt partitioning behaviour brought about by the higher temperatures and pressures of the asthenospheric source of the metasomatic melts. This is demonstrated if partition coefficients from Salters et al. (2002) [obtained for temperatures $\geq$1560°C at pressures of 2.8–3.2 GPa] are used to calculate the composition of the metasomatic melt (Fig. 7). It is also worth considering that the metasomatic melt may have been added to a protolith other than the E-DMM.

Relative to pyrolite, our metasomatized E-DMM source is enriched in Al_2O_3 ($\sim$6.0 wt.%) and CaO ($\sim$5.0 wt.%). This is the result of a large fraction of (presumably) basanitic melt being added to an already fertile peridotite. Although the fraction of added metasomatic melt can be reduced by decreasing the degree of melting needed to produce it, this causes excessive fractionations of some elements (e.g. Nb/Ta). It is also impossible to reproduce the convex-upward patterns and strong absolute concentrations of moderately incompatible elements (e.g. Hf, Sm and Ho) with small melt increments. Either the source was more enriched in Al_2O_3 and CaO than pyrolite, or metasomatic melts were added to a peridotite protolith that was already depleted in Al_2O_3 and CaO. A problem with the first alternative is that it increases the fractions of garnet and clinopyroxene in residues. This markedly increases the bulk partition coefficients of some elements (e.g. Ti, Hf and HREE) and makes the inter-element correlations in the

natural rocks difficult to reproduce by partial-melting of the same common source.

An Al_2O_3- and CaO-depleted protolith that is readily available is the sub-continental lithosphere. O'Reilly and Zhang (1995) have previously commented on correlations between the isotopic characteristics of Cainozoic basalts in eastern Australia and those of their entrained lithospheric xenoliths. Thus, O'Reilly and Zhang (1995) also argue that the compositions of magmas tend to reflect the history of the lithospheric mantle through which they pass and also interact. This history could be interpreted to include basalt source formation. Evidence which is consistent with this possibility is the experimentally determined conditions of origin for UT-70489. These lie on a continuation of the xenolith-derived lithosphere geotherm for eastern Australia and Bow Hill (Fig. 8). Thus, at the time of volcanism beneath Oatlands, conditions within the lower lithosphere were hot enough for partial-melting and magma formation to occur.

The only additional and necessary factor for lithospheric involvement in magma formation is that the lithospheric mantle beneath Oatlands did not have a previous long-term history of metasomatic enrichment. Lithospheric xenoliths without metasomatic enrichments are rare in eastern Australian Cainozoic basalts; but they do occur and have been found in volcanic centres neighbouring Oatlands (see Beyer 2002). It is possible that prior to Cainozoic volcanism, such material was more prevalent beneath eastern Australia. The alternative possibility is that magma formation occurred within the uppermost asthenosphere close to the lithosphere/asthenosphere boundary. This would independently explain the association between volcanism and metasomatism in xenoliths, but would also require the presence of depleted peridotite within the upper asthenosphere.

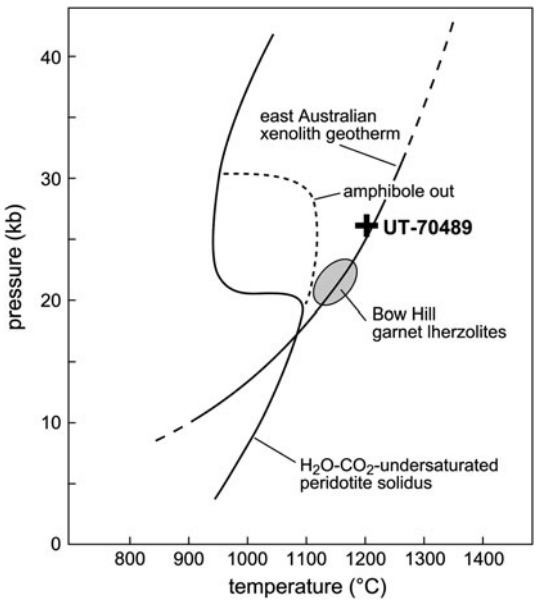

Fig. 8 Conditions of origin for UT-70489 inferred from high-pressure liquidus phase relationships (from Adam 1990). Plotted for comparison are the H_2O-CO_2-undersaturated pyrolite solidus (from Wallace and Green 1988), the eastern Australian xenolith geotherm of O'Reilly and Griffin (1985), and estimated conditions of equilibration of garnet lherzolite xenoliths from Bow Hill. Mineralogical data for the Bow Hill xenoliths came from Sutherland et al. (1984) and Adam (unpublished data). Pressures and temperatures were calculated using the formulations of Wells (1977) and Nickel and Green (1985)

The relative timing of volcanism and source formation

As we have so far described it, our metasomatic model does not require a direct temporal relationship between metasomatism and the generation of erupted magmas, but a consistent model of volcanism is much easier to produce if this was the case. This is because intraplate volcanism can be viewed as a natural consequence of two interacting phenomena. One is near-solidus melting in the asthenosphere. The other is the conductive geotherm which prevails in the lithosphere and shallow asthenosphere. As near-solidus melts ascend (presumably by vertical percolation), they encounter an increasingly sub-adiabatic geotherm which causes them to re-equilibrate and re-crystallize within overlying mantle rocks. This enriches both the new host rocks and any residual melts in incompatible elements. Tapping of the residual melts by vertically propagating fractures may then produce nephelinitic and basanitic volcanism. In other instances, upwelling of the enriched and partially molten source rocks results in decompression melting at shallower depths [a similar mechanism which links local mantle advection to melt-related buoyancy increases is described by Raddick et al. (2002)]. This produces alkali basaltic and tholeiitic volcanism.

In the case that has been described, only a single thermal event is needed to produce volcanism. Metasomatism also transfers some of the heat and fluxable components needed to produce volcanism. It is clear that at the time of volcanism at Oatlands, conditions in the lower lithosphere and/or uppermost asthenosphere were hot enough for residual metasomatic melts to persist (see Fig. 8). Another consequence of having the source remain partially molten is that the melt phase becomes a repository for volatiles, such as H_2O, CO_2 and halogens. This removes the need for intermediate storage of volatiles in mineral phases that have restrictive stability fields (e.g. amphibole, mica and carbonate). A final consideration is that the short time scales and strong element fractionations needed to produce disequilibria in the decay series of U in some young intraplate volcanics (see Thomas et al. 1999; Bourdon et al. 2003; Demidjuk et al. 2007) can be more easily explained.

Application to intraplate volcanism in other settings

Because the basalts at Oatlands share many of their essential characteristics with volcanics produced in other settings, a necessary test of any model for their origin is its ability to explain similar volcanism in different tectonic settings. A core conclusion of this present study is that, even if larger degrees of melting are ultimately involved in magma formation, the incompatible-element characteristics of intraplate basaltic magmas are primarily determined by peridotite/melt partitioning and small degrees of melting. These effects can be intensified by the influence of conductive geotherms on open-system melting processes. These conclusions make many aspects of intraplate volcanism easier to explain, although they also challenge some previously advocated models of hot-spot magma generation.

As previously mentioned, intraplate volcanism is often considered synonymous with hot-spot magmatism. However, many intraplate volcanic occurrences are lava fields, as exemplified by eastern Australia. In eastern Australia volcanism was scattered but widespread, dominantly alkaline in character and of prolonged duration. Seismic velocities beneath the eastern Australian seaboard indicate current mantle temperatures that are close to the moist MORB mantle solidus (Goes et al. 2005). Because of the rifting that produced the Tasman and Coral Seas in the late Cretaceous and early Cainozoic, combined with an earlier Mesozoic/Palaeozoic history of plate subduction, it is likely that such conditions were prevalent beneath a broad area of eastern Australia for much of the Cainozoic (see Lister and Etheridge 1989). This would be especially true if high thermal gradients were maintained by small-scale convection within the upper asthenosphere, as has been argued to occur beneath rifts and some areas of young ocean crust (see Buck 1986; Afonso et al. 2008; Zlotnik et al. 2008; Ballmer et al. 2007, 2009). As this kind of convection takes some time to develop, it might also explain why the peak in lava plains volcanism occurred some time after the opening of the Tasman and Coral Seas (see Cas 1989). If Cainozoic volcanism in eastern Australia was initiated by metasomatism (i.e. near-solidus melting) the additional thermal perturbation required to produce volcanism would have been relatively small. Thus, it would not have been difficult to produce intermittent volcanism over a large area and for a prolonged period of time.

Other examples similar to eastern Australia include Cainozoic lava fields in Vietnam, Korea, eastern China and Alaska. The volcanism in these provinces is compositionally similar to that in eastern Australia, was produced over a similar length of time and also has a scattered distribution (see Whitford-Stark 1987; Knutson et al. 1989; Chung et al. 1994; O'Reilly and Zhang 1995; Liu et al. 2001; Winer et al. 2004; Moll-Stalcup 1994, 1995; Hoang and Flower 1998; Choi et al. 2007). In addition, all of these examples occur in continental settings that are adjacent to marginal ocean basins. Thus, volcanism can be related to similar histories of plate subduction and later extension (see Chung et al. 1994; Liu et al. 2001). Intraplate volcanism is also characteristic of other extensional settings that can be either directly or indirectly related to plate boundaries. These include regions of continental rifting and collision (e.g. Kampunzu and Lubala 1991; Wilson and Downes 1991; Aldanmaz et al. 2006). Intraplate volcanism is even present in some areas of post and late arc volcanism (e.g. Thorpe 1977; Thorkelson and Smith 1989; Janousek et al. 2010). A general feature of these settings is the long time scales (equalling tens of millions of years) over which intermittent volcanism occurs.

Unlike any of the settings already described, hot spots show no evident relationship to plate boundaries, although they are more common in oceanic than continental environments. Their suggested mode of origin is also distinct (see Morgan 1971). This is generally accepted to be a rising column or 'plume' of buoyant material that ascends from deep within the mantle. On the basis of olivine thermometry for ocean island basalts (Putirka et al. 2007), it has been suggested that hot spots are indeed hot and that the mantle-plumes which produce them are hundreds of degrees hotter than the surrounding (MORB source) mantle. A problem with this proposition is that similar magmas are also produced in non-hot-spot settings, such as lava fields (see Knutson et al. 1989). In these cases magmas may be erupted sporadically and in very limited volumes for periods that vary from tens of thousands to tens of millions of years (see Johnson 1989 and references therein). This independence of scale and time is difficult to reconcile with a need for extreme temperatures, as these are difficult to localize over prolonged periods of time. In contrast, the plume-melting models of Eggins (1992b) and Wagner and Grove (1998) are in essence very little different from our own metasomatic model. All of these models involve the addition of small-degree melts to depleted peridotite and do not require extreme thermal conditions for their operation. Thus, the thermal perturbations induced by near-surface tectonic processes must be similar to those responsible for hot-spot magmatism. The source materials involved must also be similar, and thus generally distributed within the asthenospheric mantle.

A final implication of our model is that much of the melt generated by intraplate magmatism can never be erupted, but must instead be re-assimilated into the upper mantle. This is consistent with a more widespread role for migrating small-degree melts in the mantle, as independently demonstrated by the strong incompatible-element enrichments characteristic of mantle xenoliths from basalts and kimberlites (e.g. Nixon 1987 and references therein).

Alternatives to peridotite sources

Although there is some overlap, intraplate magmas are usually isotopically distinct from MORB. They are also isotopically more diverse. Because of these features, intraplate magmas must preferentially sample geochemical and isotopic heterogeneities within the MORB mantle. It has been suggested that some of these heterogeneities may be related to subducted oceanic crust (now represented by eclogite) and/or pyroxenite veins (e.g. Hofman and White 1982: Dupuy et al. 1989; Hirschmann et al. 2003; Yaxley and Sobolev 2007). The question is whether such heterogeneities are critical for the production of intraplate magmas, as suggested by Sobolev et al. (2005), or whether they are simply an additional degree of variation (geochemical noise) that is superimposed upon other more important factors? On the basis of our present investigation, we favour the latter alternative. This is because it is the dynamics of magma production, rather than source character, which is responsible for the extreme incompatible-element enrichments present in the Oatlands samples. Without their being subject to a very strong fractionation mechanism, the magmas at Oatlands should more closely resemble mid-ocean-ridge basalts (which they isotopically resemble). The nature of this fractionation is entirely consistent with peridotite/melt equilibrium.

Summary and conclusions

Although highly enriched in incompatible elements, the intraplate basalts at Oatlands have $^{87}Sr/^{86}Sr$ and $^{143}Nd/^{144}Nd$ similar to those in some incompatible-element-depleted mid-ocean ridge basalts (E-type MORB). In spite of these features, experimentally determined partition coefficients preclude a direct origin for the original magmas by partial-melting of an incompatible-element-depleted source. They nevertheless demonstrate a clear role for both mineral/melt partitioning and depleted sources in shaping the relative concentrations of incompatible elements in the Oatlands magmas. These contradictions can be reconciled if the basalts were the result of open-system melting under the influence of a sub-adiabatic geotherm. Thus, volcanism could have been initiated by near-solidus melting in the asthenosphere. As the melts ascended, they would have tended to recrystallize and accumulate within overlying mantle rocks, thereby enriching both the host rocks and any residual melts in incompatible elements. Buoyant upwelling of this partially molten material would also have resulted in decompression melting of incompatible-element-enriched peridotite at shallower depths. This explanation precludes the need for both exceptional thermal conditions and special source materials. Thus, the production of intraplate basalts in a broad range of tectonic environments becomes easier to explain, since the conditions required are either already present or easy to produce (as a consequence of either near-surface tectonics and/or deeper mantle processes). Our explanation is also consistent with a widespread role for the production, migration and re-assimilation into the mantle of small-degree melts (with intraplate volcanism being only one product of these phenomena).

Acknowledgments This research was supported by an ARC Small Grant and a Macquarie University small grant to Trevor Green. We thank Dr Norm Pearson, Suzie Elhou and Carol Conning for their assistance with the electron microprobe and LAM ICP-MS analyses. Solution ICP-MS analyses were conducted by Suzie Elhou and Peter Wieland; Sr and Nd isotopes were analysed by Peter Wieland; and Carol Lawson performed the XRF analyses of Cl and Br. This manuscript benefited from comments by Professor Sue O'Reilly, as well as reviews by Dr. Dave Draper and an unknown reviewer. This is publication number XXX in the Australian Research Council National Key Centre for the Geochemical Evolution and Metallogeny of Continents (GEMOC). This study used instrumentation funded by ARC, LIEF and DEST Systematic Infrastructure Grants, Macquarie University and Industry.

References

Adam J (1990) The geochemistry and experimental petrology of sodic alkaline basalts from Oatlands, Tasmania. J Petrol 31:1201–1223

Adam J, Green TH (2006) Trace element partitioning between mica- and amphibole-bearing garnet lherzolite and hydrous basanitic melt: 1. experimental results and the investigation of controls on partitioning behaviour. Contrib Mineral Petrol 152:1–17

Afonso JC, Zlotnik S, Fernàndez M (2008) Effects of compositional and rheological stratifications on small-scale convection under the oceans: implications for the thickness of ocean lithosphere and seafloor flattening. Geophys Res Lett 35:L20308. doi: 10.1029/2008GL035419

Albarède F (1995) Introduction to geochemical modelling. Cambridge, Cambridge University Press, p 543

Aldanmaz E, Köprübaşi N, Gürer ÖF, Kaymakçi N, Gourgaud A (2006) Geochemical constraints on the Cenozioc, OIB-type alkaline volcanic rocks of NW Turkey: implications for mantle sources and melting processes. Lithos 86:50–76

Bailey DK (1982) Mantle metasomatism—continuing chemical change within the Earth. Nature 296:525–530

Ballmer MD, van Hunen J, Ito G, Bianco TA, Tackley PJ, Bianco TA (2007) Non-hotspot volcano chains originating from small-scale sublithospheric convection. Geophysic Res Lett 34:L23310. doi: 10.1029/2007GL031636

Ballmer MD, van Hunen J, Ito G, Bianco TA, Tackley PJ (2009) Intraplate volcanism with complex age-distance patterns: a case for small-scale sublithospheric convection. Geochem Geophys Geosystems 10:Q06015. doi:10.1029/2009GC002386

Barker DS, Mitchel RH, McKay D (1987) Late Cretaceous nephelinite to phonolite magmatism in the Balcones province, Texas. Geol Soc Am Special paper 215:293–304

Berry RF, Banks MR (1985) Striations on minor faults and the structure of the Parmeener Super-group near Hobart, Tasmania. Papers Proc Royal Soc Tasmania 119:23–29

Beyer, EE (2002) Evolution of the lithosphere beneath Tasmania and western Norway. Unpublished Ph. D. thesis Macquarie University, Australia

Bourdon B, Henderson GM, Lundstrom CC, Turner SP (2003) Uranium series geochemistry. Reviews in mineralogy and geochemistry, vol 52. Geochemical Society-Mineralogical Society of America, Washington, p 656

Buck R (1986) Small scale convection induced by passive rifting: the cause for uplift of rift shoulders. Earth Planet Sci Lett 77:362–372

Cas RAF (1989) Physical volcanology. In: Johnson RW (ed) Intraplate volcanism in eastern Australia and New Zealand, chapter 2. Cambridge University Press, Cambridge, pp 55–83

Chen C-Y, Frey FA, Rhodes JM, Garcia MO (1996) Temporal geochemical evolution of Kilauea Volcano: composition of Hilina and Puna basalt. In: Basu A, Hart S (eds) Earth processes: reading the isotopic code. Geophysical Monograph, American Geophysical Union 95:161–181

Choi SH, Mukasa SB, Kwon S-T, Andronikov AV (2007) Sr, Nd, Pb and Hf isotopic compositions of late Cenozoic alkali basalts in South Korea: evidence for mixing between the two dominant asthenospheric mantle domains beneath East Asia. Chemical Geology 232:134–151

Chung S-L, Sun S-S, Tu K, Chen C-H, Lee C-Y (1994) Late Cainozoic basaltic volcanism around the Taiwan Strait, SE China: product of lithosphere-asthenosphere interaction during continental extension. Chemical Geology 112:1–20

Clague DA, Frey FA (1982) Petrology and trace element geochemistry of the Honolulu Volcanics, Oahu: implications for the oceanic mantle below Hawaii. J Petrol 23(3):447–504

Cohen AS, O'Nions RK, Kurz MD (1996) Chemical and isotopic variations in Mauna Loa tholeiites. Earth Planet Sci Lett 143:111–124

Demidjuk Z, Turner S, Sandiford M, George R, Foden J, Etheridge M (2007) U-series isotope and geodynamic constraints on mantle melting processes beneath the Newer Volcanic Province in South Australia. Earth Planet Sci Lett 261:517–533

Duncan RA, McDougall I (1989) Volcanic time-space relationships. In: Johnson RW (ed) Intraplate volcanism in eastern Australia and New Zealand. Cambridge University Press, Cambridge, pp 43–53

Dupuy C, Barsczus H, Dostal J, Vidal P, Liotard J (1989) Subducted and recycled lithosphere as the mantle source of ocean island basalts from southern Polynesia, Central Pacific. Earth Planet Sci Lett 114:477–489

Eggins SM (1992a) Petrogenesis of Hawaiian tholeiites: 1, phase equilibria constraints. Contrib Mineral Petrol 110:387–397

Eggins SM (1992b) Petrogenesis of Hawaiian tholeiites: 2, aspects of dynamic melt segregation. Contrib Mineral Petrol 110:398–410

Eggins SM, Woodhead JD, Kinsley LPJ, Mortimer GE, Sylvester P, McCulloch MT, Hergt JM, Handler MR (1997) A simple method for the precise determination of $\geq$40 trace elements in geological samples by ICPMS using enriched isotope internal standardization. Chem Geol 134:311–326

Ferguson EM, Klein EM (1993) Fresh basalts from the Pacific-Antarctic Ridge extend the Pacific geochemical province. Nature 366:330–333

Frey FA, Green DH, Roy SD (1978) Integrated models of basalt petrogenesis: a study of quartz tholeiites to olivine melilitites from South Eastern Australia utilizing geochemical and experimental data. J Petrol 19:463–513

Frey FA, Clague D, Mahoney JJ, Sinton JM (2000) Volcanism at the edge of the Hawaiian plume: petrogenesis of submarine alkalic lavas from the North Arch volcanic field. J Petrol 41:667–691

Goes S, Simons FJ, Yoshizawa K (2005) Seismic constraints on temperature of the Australian uppermost mantle. Earth Planet Sci Lett 236:227–237

Green DH (1989) Experimental petrology. In: Johnson RW (ed) Intraplate volcanism in eastern Australia and New Zealand, chapter 7.5. Cambridge University Press, Cambridge, pp 321–324

Green DH, Liebermann RC (1976) Phase equilibria and elastic properties of a pyrolite model for the oceanic upper mantle. Tectonophysics 32:61–92

Green DH, Ringwood AE (1967) The genesis of basaltic magmas. Contrib Mineral Petrol 15:103–190

Halliday AN, Lee D-C, Tommasini S, Davies GR, Paslick CR, Fitton JG, James DE (1995) Incompatible trace elements in OIB and MORB and source enrichment in the sub-oceanic mantle. Earth Planet Sci Lett 133:379–395

Hirschman MM, Kogiso T, Baker MB, Stolper EM (2003) Alkalic magmas generated by partial melting of garnet pyroxenite. Geology 31:481–484

Hoang N, Flower M (1998) Petrogenesis of Cenozoic basalts from Vietnam: implications for origins of a "diffuse igneous province". J Petrol 39:369–395

Hofman AW, White WM (1982) Mantle plumes from ancient oceanic crust. Earth Planet Sci Lett 57:421–436

Hofmann AW, Feigenson MD (1983) Case studies on the origin of basalt: I. theory and reassessment of Grenada basalts. Contrib Mineral Petrol 84:382–389

Ito E, White WM, Gopel C (1987) The O, Sr, Nd and Pb isotope geochemistry of MORB. Chem Geol 62:157–176

Janousek V, Erban V, Holub FV, Magna T, Bellon H, Mlčoch B, Wiechert U, Rapprich V (2010) Geochemistry and genesis of behind-arc basaltic lavas from eastern Nicaragua. J Vol Geotherm Res 192:232–256

Johnson RW (1989) Intraplate volcanism in Eastern Australia and New Zealand. Cambridge University Press, Cambridge

Kamenetsky VS, Everard JL, Crawford AJ, Varne R, Eggins SM, Lanyon R (2000) Enriched end-member of primitive MORB melts: petrology and geochemistry of glasses from Macquarie Island (SW Pacific). J Petrol 41:411–430

Kampunzu AB, Lubala RT (1991) Magmatism in extensional structural settings: the Phanerozoic African plate. Springer-Verlag, Berlin, p 637

Knutson J, Sun S-S, Ewart A (1989) In: Johnson RW (ed) Intraplate Volcanism in eastern Australia and New Zealand. Cambridge University Press, Cambridge, chapter 7.4 pp. 313–320

Lister GS, Etheridge MA (1989) Detachment models for uplift and volcanism in the eastern highlands, and their application to the origin of passive margin mountains. In: Johnson RW (ed) Intraplate volcanism in eastern Australia and New Zealand. chapter 7.3. Cambridge University Press, Cambridge, pp 297–307

Liu J, Han J, Fyfe S (2001) Cenozoic episodic volcanism and continental rifting in northeast China and possible link to Japan Sea development as revealed by K-Ar geochronology. Tectonophysics 339:385–401

McDonough WF, Sun S-S (1995) The composition of the Earth. Chem Geol 120:223–253

McDonough WF, McCulloch MT, Sun S-S (1985) Isotopic and geochemical systematics in Tertiary-Recent basalts from southeastern Australia and implications for the evolution of the sub-continental lithosphere. Geochim Cosmochim Acta 49: 2051–2067

McKenzie DP (1984) The generation and compaction of partially molten rock. J Petrol 25:713–765

Moll-Stalcup EJ (1994) Latest Cretaceous and Cenozoic magmatism in mainland Alaska. In: Plafker G, Berg HC (eds) The geology of Alaska. The geology of North America, vol G-1. Geological Society of America, Boulder, pp 589–619

Moll-Stalcup EJ (1995) The origin of the Bering Sea basalt province, western Alaska. In: Simakov, KV, Thurston DK (eds) 1994 Proceedings: International conference on Arctic Margins.

Russian Academy of Sciences Far East Branch North East Science Center, Magadan, Russia, pp. 113–123
Morgan WJ (1971) Convection plumes in the lower mantle. Nature 230:42–43
Nickel KG, Green DH (1985) Empirical geothermobarometry for garnet peridotites and implications for the nature of the lithosphere, kimberlites and diamonds. Earth Planet Sci Lett 73:158–170
Nixon PH (1987) Mantle xenoliths. John Wiley & Sons, New York
O'Reilly SY, Griffin WL (1985) A xenolith derived geotherm for southeastern Australia and its geophysical implications. Tectonophysics 111:41–63
O'Reilly SY, Zhang M (1995) Geochemical characteristics of lava-field basalts from eastern Australia and inferred sources: connections with the subcontinental lithospheric mantle? Contrib Mineral Petrol 121:148–170
Ormerod DS, Rogers NW, Hawkesworth CJ (1991) Melting in the lithospheric mantle: inverse modelling of alkali-olivine basalts from the Big Pine Volcanic Field, California. Contrib Mineral Petrol 108:305–317
Pfänder JA, Münker C, Stracke A, Mezger K (2007) Nb/Ta and Zr/Hf in ocean island basalts–Implications for crust-mantle differentiation and the fate of Nb. Earth Planet Sci Lett 254:158–172
Pilet S, Hernandez J, Sylvester P, Poujol M (2005) The metasomatic alternative for ocean island basalt chemical heterogeneity. Earth Planet Sci Lett 236:148–166
Pin C, Francisco J, Zalduegui S (1997) Sequential separation of light rare-earth elements, thorium and uranium by miniaturized extraction chromatography: application to isotopic analyses of silicate rocks. Anal Chim Acta 339:79–89
Putirka KD, Pelt M, Ryerson FJ, Jackson MG (2007) Ambient and excess mantle temperatures, olivine thermometry, and active vs. passive upwelling. Chem Geol 241:177–206
Pyle DG, Christie DM, Mahoney JJ, Duncan RA (1995) Geochemistry and geochronology of ancient southeast Indian and southwest Pacific seafloor. J Geophys Res 100:22261–22282
Raddick MJ, Parmentier EM, Scheirer (2002) Buoyant decompression melting: a possible mechanism for intraplate volcanism. J Geophys Res 107(B10):228. doi:10.1029/2001JB000617
Richter FM (1986) Simple models for trace element fractionation during melt segregation. Earth Planet Sci Lett 77:333–344
Ringwood TE (1966) The chemical composition and origin of the earth. In: Hurley PM (ed) Advances in earth science, pp 287–356
Roden MF, Frey FA, Clague DA (1984) Geochemistry of tholeiitic and alkalic lavas from the Koolau Range, Oahu, Hawaii: implications for Hawaiian volcanism. Earth Planet Sci Lett 69:141–158
Roeder PL, Emslie RF (1970) Olivine-liquid equilibria. Contrib Mineral Petrol 29:275–289
Salters VJM, Longhi JE, Bizimis M (2002) Near mantle solidus trace element partitioning at pressures up to 3.4 GPa. Geochem. Geophys. Geosyst 3 (paper number 2001GC000148)
Schminke HU (1982) Volcanic and chemical evolution of the Canary Islands. In: von Rad U, Hinz K, Sarnthein M, Seibold E (eds) Geology of the Northwest African continental margin. Heidelberg, Springer Verlag, pp 273–306
Shaw D (2006) Trace elements in Magmas. Cambridge University Press, Cambridge
Sobolev AV, Hofmann AW, Sobolev SV, Nikogosian IK (2005) An olivine-free mantle source of Hawaiian shield basalts. Nature 434:590–597
Sun S-S, Hanson GN (1975) Origin of Ross Island basanitoids and limitations upon the heterogeneity of mantle sources for alkali basalts and nephelinites. Contrib Mineral Petrol 52:77–106
Sun S-S, McDonough WF (1989) Chemical and isotopic systematics of oceanic basalts: implications for mantle composition and processes. Geol Soc Special Publication 42:313–345
Sutherland FL (1984) Cainozoic basalts. In Forsyth SM (ed) Geological atlas 1:50 000 series sheet, Oatlands. Geological survey of Tasmanian—Explanatory report
Sutherland FL, Wellman P (1986) Potassium-argon ages of Tertiary volcanic rocks, Tasmania. Pap Proc R Soc Tasmania 120:77–86
Sutherland FL, Hollis JD, Barron LM (1984) Garnet lherzolite and other inclusions from a basalt flow, Bow Hill, Tasmania: Proceedings 3rd Int Kimberlite Conference vol 2, pp 145–160 Elsevier, Amsterdam
Thomas LE, Hawkesworth CJ, Van Calsteren P, Turner SP, Rogers NW (1999) Melt generation beneath ocean islands: a U-Th-Ra isotope study from Lanzarote in the Canary Islands. Geochim Cosmochim Acta 63:4081–4099
Thorkelson DJ, Smith AD (1989) Arc and intraplate volcanism in the Spences Bridge Group: implications for Cretaceous tectonics in the Canadian Cordillera. Geology 17:1093–1096
Thorpe RS (1977) Tectonic significance of alkaline volcanism in Mexico. Tectonophysics 40:19–26
Varne R (1970) Hornblende Lherzolite and the upper mantle. Contrib Mineral Petrol 27:45–51
Wagner TP, Grove TL (1998) Melt/harzburgite reaction in the petrogenesis of tholeiitic magma from Kilauea volcano, Hawaii. Contrib Mineral Petrol 131:1–12
Wallace ME, Green DH (1988) An experimental determination of primary carbonatite magma composition. Nature 335:343–346
Weaver BL (1991) The origin of ocean island basalt end-member compositions: trace element and isotope constraints. Earth Planet Sci Lett 104:381–397
Wedepohl KH (1985) Origin of the tertiary basaltic volcanism in the northern Hessian Depression. Contribs Mineral Petrol 89: 122–143
Wells PRA (1977) Pyroxene thermometry in complex and simple systems. Contrib Mineral Petrol 62:129–139
Whitford-Stark JL (1987) A survey of Cainozoic volcanism on mainland Asia. Geol Soc America Special Paper 213
Wilkinson JFG, Hensel HD (1991) An analcime mugearite-megacryst association from north-eastern New South Wales: implications for high-pressure amphibole-dominated fractionation of alkaline magmas. Contrib Mineral Petrol 109:240–251
Wilson M, Downes M (1991) Tertiary-Quaternary extension-related alkaline magmatism in western and central Europe. Journal of Petrology 32:811–849
Winer GS, Feeley TC, Cosca MA (2004) Basaltic volcanism in the Bering Sea: geochronology and volcanic evolution of St. Paul Island, Pribilof Islands, Alaska. J Vol Geotherm Res 134:277–301
Workman RK, Hart SR (2005) Major and trace element composition of the depleted MORB mantle (DMM). Earth Planet Sci Lett 231:53–72
Wright TL (1984) Origin of Hawaiian tholeiites: a metasomatic model. J Geophys Res 89-B5:3233–3252
Yaxley GM, Sobolev AV (2007) High-pressure partial melting of gabbro and its role in the Hawaiian magma source. Contrib Mineral Petrol 154:371–383
Zhang M, O'Reilly SY (1997) Multiple source rocks for basaltic rocks from Dubbo, eastern Australia: geochemical evidence for plume-lithospheric mantle interaction. Chem Geol 136:33–54
Zhang M, Stephenson PJ, O'Reilly SY, McCulloch MT, Norman M (2001) Petrogenesis and geodynamic implications of late Cainozoic basalts in North Queensland, Australia: trace-element and Sr-Nd-Pb isotope evidence. J Petrol 42:685–719
Zindler A, Hart S (1986) Chemical geodynamics. An Rev Earth Planet Sci Lett 14:493–571
Zlotnik S, Alfonso JC, Díez P, Fernández M (2008) Small-scale gravitational instabilities under the oceans: implications for the evolution of oceanic lithosphere and its expression in geophysical observables. Philos Mag 88:3197–3217